PHYSICAL REVIEW D **92,** 094028 (2015)

QCD corrections to ZZ production in gluon fusion at the LHC

Fabrizio Caola,[1,*] Kirill Melnikov,[2,†] Raoul Röntsch,[3,‡] and Lorenzo Tancredi[2,§]

[1]*CERN Theory Division, CGH-1211, Geneva 23, Switzerland*
[2]*Institute for Theoretical Particle Physics, KIT, D-76128 Karlsruhe, Germany*
[3]*Department of Theoretical Physics, Fermilab, Batavia, Illinois 60510, USA*

(Received 29 September 2015; published 23 November 2015)

We compute the next-to-leading-order QCD corrections to the production of two Z-bosons in the annihilation of two gluons at the LHC. Being enhanced by a large gluon flux, these corrections provide a distinct and, potentially, the dominant part of the N^{3}LO QCD contributions to Z-pair production in proton collisions. The $gg \to ZZ$ annihilation is a loop-induced process that receives the dominant contribution from loops of five light quarks, that are included in our computation in the massless approximation. We find that QCD corrections increase the $gg \to ZZ$ production cross section by $\mathcal{O}(50\%–100\%)$ depending on the values of the renormalization and factorization scales used in the leading-order computation and the collider energy. The large corrections to the $gg \to ZZ$ channel increase the $pp \to ZZ$ cross section by about 6% to 8%, exceeding the estimated theoretical uncertainty of the recent next-to-next-to-leading-order QCD calculation.

DOI: 10.1103/PhysRevD.92.094028 PACS numbers: 12.38.-t, 12.38.Bx

I. INTRODUCTION

Production of pairs of vector bosons in proton collisions is one of the most interesting processes studied by ATLAS and CMS during the LHC Run I [1–3]. Indeed, $pp \to ZZ$, $pp \to W^+W^-$, and $pp \to \gamma\gamma$ were instrumental for the discovery of the Higgs boson. As the focus of Higgs physics shifts from the discovery to precision studies of the Higgs boson properties, diboson production processes become essential for constraining anomalous Higgs boson couplings, for measuring the quantum numbers of the Higgs boson and for studying the Higgs boson width; see Refs. [4–7]. Additionally, these processes provide important tests of our understanding of the Standard Model and can be used to constrain anomalous electroweak gauge boson couplings.

Production of electroweak gauge boson pairs occurs mainly due to quark-antiquark annihilation $q\bar{q} \to V_1V_2$. This contribution is known through next-to-next-to-leading order (NNLO) in perturbative QCD [8–13]. However, as was pointed out in Refs. [14–16], there is a sizable contribution from the gluon annihilation channel $gg \to V_1V_2$, the significance of which depends on the selection cuts. For example, aggressive cuts applied to $pp \to W^+W^-$ to separate the Higgs boson signal from the continuum background can increase the fraction of gluon fusion events in the background sample [17]. Since $gg \to V_1V_2$ is a one-loop process and since production of electroweak boson pairs at leading order (LO) occurs only in the $q\bar{q}$ channel, the gluon fusion contribution to $pp \to V_1V_2$ through NNLO only needs to be known at leading order, i.e. the one-loop approximation. Thus, all existing numerical estimates of the significance of the gluon fusion mechanism in weak boson pair production ignore radiative corrections to $gg \to ZZ$ that are, potentially, quite large [18]. The need to have an accurate estimate of QCD corrections to gluon fusion processes for the Higgs width [19,20] and generic off-shell measurements [21–23] was strongly emphasized in Ref. [7].

In this paper, we will focus on the calculation of the next-to-leading-order (NLO) QCD corrections to the gluon fusion contribution to the $pp \to ZZ$ process. The largest contribution to $gg \to ZZ$ comes from quarks of the first two generations; these quarks can be taken to be massless. The situation is more complicated for quarks of the third generation. Ideally, we would like to include the (massless) bottom-quark contribution and ignore the contribution of the massive top quark since, at leading order, the top-quark contributions change the cross section by only about 1% (cf. Refs. [24,25]).[1] We can separate bottom and top contributions everywhere except in triangle diagrams that involve anomalous correlators of vector and axial currents. In these triangle diagrams, when bottom and top contributions are combined, the residual contributions are suppressed by the top-quark mass, provided that we can assume it to be larger than any other energy scale in the problem. Unfortunately, in these diagrams top and bottom contributions cannot be separated because the resulting theory is anomalous. To deal with this issue, we adopt the

*fabrizio.caola@cern.ch
†kirill.melnikov@kit.edu
‡rontsch@fnal.gov
§lorenzo.tancredi@kit.edu

[1]Contribution of the top-quark loop becomes non-negligible in the region of high four-lepton invariant masses $m_{4l} > 2m_t$.

following strategy: we include quarks of the first two generations and the b-quark in our calculation in the massless approximation, and we neglect all triangle diagrams of which the contribution is then naturally associated with the quark contributions to the $gg \to ZZ$ process. We note that the evaluation of the NLO QCD corrections to the top-quark mediated contribution to the $gg \to ZZ$ process is not yet possible because the relevant two-loop amplitudes are not available. However, such contributions were recently studied in Ref. [26] in the approximation of a very large mass of the top quark. In that calculation quite large QCD corrections were found.

Computing NLO QCD corrections to the $gg \to ZZ$ process is challenging because it is loop induced. For this reason, the NLO QCD computation requires two-loop virtual matrix elements for $gg \to ZZ$ and one-loop matrix elements for $gg \to ZZg$ processes. The recent progress in calculating two-loop integrals with two massless and two massive external lines [27–32] made it possible to compute the required two-loop scattering amplitudes. Such amplitudes were calculated recently for $q\bar{q} \to V_1V_2$ [32,33] and $gg \to V_1V_2$ [34,35] processes.

The second ingredient that we need is the $gg \to ZZg$ amplitude. Since this is a one-loop amplitude, it can be calculated in a relatively standard way, at least as a matter of principle. In fact, such calculations were performed in the past [36,37] and used to predict the production cross section for $pp \to ZZ + j$. Automatic tools for one-loop computations can also deal with this process [38–40]. Nevertheless, it is a nontrivial computation since, if we aim at calculating the NLO QCD corrections to $gg \to ZZ \to 4l$, we require the fast and stable calculation of helicity amplitudes for the $gg \to ZZg$ process that includes decays of Z-bosons to leptons and can be extrapolated to soft and collinear kinematics of the final state gluon. Because of that, we decided to construct our own implementation of the scattering amplitude for $gg \to ZZg$ using the unitarity methods [41–45].[2]

The paper is organized as follows. In Sec. II we present a brief review of the calculation of the two-loop scattering amplitude for the $gg \to ZZ$ process. In Sec. III we discuss the calculation of the one-loop helicity amplitudes for $gg \to ZZg$ and present numerical results for a kinematic point. In Sec. IV we present numerical results for the $gg \to ZZ$ contribution to the $pp \to ZZ$ process at 8 and 13 TeV LHC at leading and next-to-leading orders in perturbative QCD. We conclude in Sec. V.

II. TWO-LOOP SCATTERING AMPLITUDES FOR $gg \to ZZ$

We start with a brief discussion of the two-loop scattering amplitudes for the $gg \to ZZ$ process. Helicity amplitudes for this process were recently computed in Refs. [34,35]. In these references, each of the two independent helicity amplitudes for the process $gg \to ZZ \to 4l$ was written as linear combinations of nine form factors that depend on the Mandelstam invariants of the "prompt" process $gg \to ZZ$ and the invariant masses of the two Z-bosons. The form factors are expressed in terms of polylogarithmic functions, including both ordinary and Goncharov polylogarithms.

In this paper we use the results of Ref. [35] which are implemented in a C++ code that can produce numerical results with arbitrary precision. To detect possible numerical instabilities, the code compares numerical evaluations obtained with different (double, quadruple, and, if required, arbitrary) precision settings. If the results differ beyond a chosen tolerance, the precision is automatically increased. Of course, switching to arbitrary precision increases the evaluation time substantially. Fortunately, we found that for phenomenologically relevant situations the number of points where the code switches to arbitrary precision is negligible. Such points originate from kinematic regions where the two Z-bosons have either vanishing kinetic energies or vanishing transverse momenta. The amplitude squared is integrable in both of these regions, but, in practice, it can become numerically unstable. Since the contribution of these regions to the $gg \to ZZ$ cross section is relatively small, cutting them away, in principle, leads to an opportunity to perform stable numerical integration of the two-loop virtual correction over the four-lepton phase space, resorting to quadruple precision only. However, we found that the improvement in performance achieved by cutting away the problematic regions is rather limited, so we used the default arbitrary precision implementation of the two-loop amplitude in practice.

Since the $gg \to ZZ$ amplitude is one of the most complicated amplitudes that are currently known analytically, it is interesting to point out that the required evaluation times are acceptable for phenomenological needs. Indeed, calculation of all helicity amplitudes requires about 2 s per phase-space point in quadruple precision, and, since the phase-space for $gg \to ZZ$ is relatively simple, one does not need an excessively large number of points to sample it with good precision.

For further reference we provide numerical results for the finite remainder of the one- and two-loop scattering amplitudes defined in the q_t-subtraction scheme; see Ref. [35]. The numerical results are presented for the choice of the renormalization scale $\mu = \sqrt{s}$, where s is the partonic center-of-mass energy squared. The q_t-subtraction scheme [48] is discussed in detail in Ref. [49]. We consider the kinematical point

$$g(p_1) + g(p_2) \to (Z/\gamma)(p_{34}) + (Z/\gamma)(p_{56}) \to e^-(p_3) + e^+(p_4) + \mu^-(p_5) + \mu^+(p_6)$$

with (in GeV units)

[2]For recent reviews, see Refs. [46,47].

$$
\begin{aligned}
p_1 &= (99.5173068698129, 99.5173068698129, 0, 0),\\
p_2 &= (99.5173068698129, -99.5173068698129, 0, 0),\\
p_3 &= (45.1400347869485, 43.4878610174890, -9.85307698310431, 7.02463939683013),\\
p_4 &= (55.6586029753540, -27.4053916434553, 48.1951275617684, 4.90451560725290),\\
p_5 &= (36.2015682945089, 34.5902512456859, -8.01242197258994, 7.06180995747356),\\
p_6 &= (62.0344076828144, -50.6727206197196, -30.3296286060742, -18.9909649615566)
\end{aligned} \tag{1}
$$

and define a normalized amplitude through the following equation:

$$
d\sigma_{gg\to(Z/\gamma)(Z/\gamma)\to 4l} = \frac{(N_c^2-1)}{512s}\times 10^{-6}\times \sum_{\lambda_1,\lambda_2,\lambda_e,\lambda_\mu} |A(1_g^{\lambda_1}, 2_g^{\lambda_2}; 3_{e^-}^{\lambda_e}, 4_{e^+}^{-\lambda_e}, 5_{\mu^-}^{\lambda_\mu}, 6_{\mu^+}^{-\lambda_\mu})|^2 d\mathrm{LIPS}_4. \tag{2}
$$

Note that in Eq. (2) all the color factors have been factored out, and $d\mathrm{LIPS}_4$ is the standard Lorentz-invariant phase space of the four final leptons. The color-stripped amplitude admits an expansion in the strong coupling constant

$$
\begin{aligned}
A(1_g^{\lambda_1}, 2_g^{\lambda_2}; 3_{e^-}^{\lambda_e}, 4_{e^+}^{-\lambda_e}, 5_{\mu^-}^{\lambda_\mu}, 6_{\mu^+}^{-\lambda_\mu}) = \left(\frac{\alpha_s(\mu)}{2\pi}\right)\Bigg[&\mathcal{A}_{1l}(1_g^{\lambda_1}, 2_g^{\lambda_2}; 3_{e^-}^{\lambda_e}, 4_{e^+}^{-\lambda_e}, 5_{\mu^-}^{\lambda_\mu}, 6_{\mu^+}^{-\lambda_\mu})\\
&+\left(\frac{\alpha_s(\mu)}{2\pi}\right)\mathcal{A}_{2l}(1_g^{\lambda_1}, 2_g^{\lambda_2}; 3_{e^-}^{\lambda_e}, 4_{e^+}^{-\lambda_e}, 5_{\mu^-}^{\lambda_\mu}, 6_{\mu^+}^{-\lambda_\mu}) + \mathcal{O}(\alpha_s^2)\Bigg].
\end{aligned} \tag{3}
$$

Numerical results for the two independent helicity amplitudes at one and two loops are given in Table I. We emphasize that the results in Table I are given in the q_t-subtraction scheme, cf. Ref. [35].

III. ONE-LOOP SCATTERING AMPLITUDE $0 \to gggZZ$

In this section, we discuss the computation of the one-loop scattering amplitude required for the calculation of the inelastic process $gg \to ZZ + g$.[3] To this end, we consider the process $0 \to g(p_1)g(p_2)g(p_3)Z(p_{45})Z(p_{67})$. Decays of the Z-bosons are allowed, but, since we are interested in the on-shell production of the two Z-bosons, we do not include single resonant diagrams where one of the Z-bosons is emitted from the decay products of the other one; see Fig. 1. We will refer to the decay products of the Z-boson with momentum p_{45} as the electron and the positron with momenta p_4 and p_5 and to the decay products of the Z-boson with momentum p_{67} as the muon and the anti-muon with momenta p_6 and p_7, respectively. All leptons are taken to be massless. Since helicities of massless leptons are conserved, we only need to specify helicities of the final state leptons e^- and μ^-; the allowed helicities of the positron and the antimuon in the final state are then automatically fixed.

[3]To simplify the notation, in this section we do not consider photon-mediated four-lepton amplitudes. For phenomenological results discussed in Sec. IV, we consider the full $gg \to (Z/\gamma)(Z/\gamma) + g$ amplitude.

We write the interaction vertex of the Z-boson and a fermion pair as

$$
\begin{aligned}
Z\bar{f}\gamma_\mu f \in\ & g_{L,f}\frac{\gamma_\mu(1+\gamma_5)}{2} + g_{R,f}\frac{\gamma_\mu(1-\gamma_5)}{2},\\
& f \in (l, q).
\end{aligned} \tag{4}
$$

The left and right couplings for leptons and quarks are given by an identical formula,

$$
g_{L(R),f} = \frac{V_f \pm A_f}{\cos\theta_W}, \tag{5}
$$

where we use *i)* $V_l = -1/2 + 2\sin^2\theta_W$, $A_l = -1/2$ for charged leptons; *ii)* $V_u = 1/2 - 4/3\sin^2\theta_W$, $A_u = 1/2$ for up-type quarks; and *iii)* $V_d = -1/2 + 2/3\sin^2\theta_W$, $A_d = 1/2$ for down-type quarks.

The $0 \to gggZZ$ scattering amplitude can be written as a sum of two terms,

$$
\mathcal{A}^{ZZ} = g_s^3 g_W^4(\mathrm{Tr}[t^{a_1}t^{a_2}t^{a_3}]A_{123}^{ZZ} + \mathrm{Tr}[t^{a_1}t^{a_3}t^{a_2}]A_{132}^{ZZ}), \tag{6}
$$

with $\mathrm{Tr}(t^a t^b) = \delta^{ab}/2$. The two color-ordered amplitudes, stripped of their couplings to leptons and quarks, are defined as

$$
\begin{aligned}
A_{\mathrm{ijk}}^{ZZ} = C_{\lambda_e,e}C_{\lambda_\mu,\mu}(&g_{LL}^{ZZ}\mathcal{A}_{\mathrm{ijk}}^{LL}(\lambda_i,\lambda_j,\lambda_k;\lambda_e,\lambda_\mu)\\
&+ g_{RR}^{ZZ}\mathcal{A}_{\mathrm{ijk}}^{RR}(\lambda_i,\lambda_j,\lambda_k;\lambda_e,\lambda_\mu)).
\end{aligned} \tag{7}
$$

TABLE I. Results (in GeV^{-2}) for the normalized q_t remainder of one- and two-loop amplitudes for different choices of gluon and lepton helicities, evaluated at the scale $\mu = \sqrt{s}$. See the text for details.

Helicity amplitude	1 loop	2 loops
$\mathcal{A}(1^-, 2^-; 3^-, 4^+, 5^-, 6^+)$	$-3.6020208 - 0.80680028i$	$-87.785548 + 35.086257i$
$\mathcal{A}(1^-, 2^+; 3^-, 4^+, 5^-, 6^+)$	$+0.2507409 + 0.38426042i$	$+18.585086 + 7.5961902i$

In Eq. (7) we introduced

$$C_{\lambda,l} = D_Z(m_{ll}^2)(g_{L,l}\delta_{\lambda,-} + g_{R,l}\delta_{\lambda,+}), \tag{8}$$

where $D_Z(s)$ is the function related to the Breit–Wigner propagator $D_Z(s) = s/(s - M_Z^2 + iM_Z\Gamma_Z)$. The couplings g_{LL}^{ZZ} and g_{RR}^{ZZ} are expressed through Z-boson couplings to quarks propagating in the loops,

$$g_{LL}^{ZZ} = \sum_q g_{L,q}^2,$$
$$g_{RR}^{ZZ} = \sum_q g_{R,q}^2. \tag{9}$$

Given these definitions, it is easy to see that the helicity amplitudes $\mathcal{A}_{\mathrm{ijk}}^{LL,RR}(\lambda_i, \lambda_j, \lambda_k; \lambda_e, \lambda_\mu)$ can be calculated for *vector* couplings of Z-bosons to leptons and quarks, provided that one keeps left-handed (right-handed) quarks propagating clockwise in the fermion loop. This is a natural separation if the scattering amplitudes are computed using the unitarity methods [41–45]. There is a useful relation between left- and right-handed helicity amplitudes for two orderings of external gluons,

$$\mathcal{A}_{132}^{LL}(\lambda_1, \lambda_3, \lambda_2; \lambda_e, \lambda_\mu) = -\mathcal{A}_{123}^{RR}(\lambda_1, \lambda_2, \lambda_3; \lambda_e, \lambda_\mu),$$
$$\mathcal{A}_{132}^{RR}(\lambda_1, \lambda_3, \lambda_2; \lambda_e, \lambda_\mu) = -\mathcal{A}_{123}^{LL}(\lambda_1, \lambda_2, \lambda_3; \lambda_e, \lambda_\mu). \tag{10}$$

These equations suggest that it is sufficient to compute LL and RR amplitudes for a single ordering; once this is done, all relevant amplitudes for the second ordering can be constructed. Finally, we emphasize that we exclude the Breit–Wigner factor[4] for the Z-bosons from the definition of the color-ordered helicity amplitudes, but we include the $1/s$ factor in its place; this can be clearly seen from the definition of the $D_Z(s)$ function in Eq. (8).

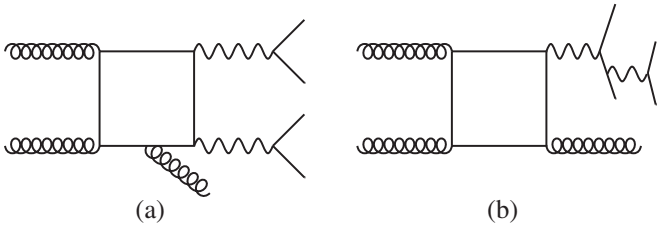

FIG. 1. Representative Feynman diagrams for the $0 \to gggZ(\to e^-e^+)Z(\to \mu^-\mu^+)$ amplitude. *Double resonant* diagrams (a) are relevant for both the on-shell and the off-shell production. *Single resonant* diagrams (b) are only relevant for the off-shell production and are not included in our computation. See the text for details.

It is well known that any one-loop amplitude can be written as a linear combination of one-loop scalar integrals that include four-, three-, and two-point functions and a rational part

$$\mathcal{A}_{\mathrm{ijk}}^{LL,RR}(\lambda_i, \lambda_j, \lambda_k; \lambda_e, \lambda_\mu) = \sum c_i^{LL,RR} I_i + R^{LL,RR}, \tag{11}$$

The coefficients c_i in the above equation, as well as the rational part, can be calculated using unitarity methods.

The idea of the unitarity method is that one can calculate the different discontinuities of the left- and right-hand sides of Eq. (11) and then combine them in such a way that coefficients c_i are extracted algebraically. Calculation of the reduction coefficients and the rational part can be performed either analytically or numerically. In this paper, we use a mixed approach. We compute the coefficients c_i using numerical four-dimensional unitarity introduced in Ref. [44]. The rational part, on the other hand, is computed analytically using the method described in Refs. [50,51]. Technical details about the unitarity methods used for one-loop computations in QCD can be found in Ref. [46].

From the point of view of the unitarity methods, the peculiarity of $0 \to gggZZ$ process is that it involves two colorless particles, making full color ordering for scattering amplitudes impossible. This has the following implications. Any unitarity computation starts with the list of independent "parent diagrams" that are subsequently cut into on-shell scattering amplitudes. Although parent diagrams are independent by construction, not all their cuts are, if permutations of external particles are allowed. The challenge, therefore, is to start with the parent diagrams, write down all the cuts that they might have, and then exclude all the cuts that are not independent. This issue was successfully dealt with in the context of many recent calculations of one-loop scattering amplitudes for quarks, gluons, and

[4]As we mentioned earlier, we are interested in the on-shell production of the two Z-bosons in this paper. However, we construct the relevant piece of the $gg \to ZZ$ amplitude in full generality, including Breit–Wigner propagators for the Z-bosons, to enable its later use to study QCD corrections to the $gg \to ZZ^*$ process.

TABLE II. Results (in GeV^{-3}) for normalized color-ordered amplitudes for the $0 \to ggg Z(e^+e^-)Z(\mu^+\mu^-)$ process, for different choices of gluon and lepton helicities. See the text for details.

Helicity	LL	RR
$\tilde{\mathcal{A}}_{123}(+,+,+;-,-)$	$-42.714233 + 117.60020i$	$-138.32358 + 139.68765i$
$\tilde{\mathcal{A}}_{123}(+,+,-;-,-)$	$+134.26016 + 161.13392i$	$+138.09750 + 188.27580i$
$\tilde{\mathcal{A}}_{123}(-,-,+;-,+)$	$-32.287418 + 2.1139258i$	$-31.55258 + 32.433444i$

vector bosons; see e.g. Refs. [52–55]. In this paper, we construct the independent set of unitarity cuts following the methodology explained in those references.

After identifying independent cuts, we find 39 quadruple, 45 triple, and 18 double cuts. There are no single-line cuts since internal fermions in our calculation are massless. Each of these cuts is described by a product of tree-level color-ordered amplitudes. The required helicity amplitudes include $\bar{q}gq$, $\bar{q}Zq$, $\bar{q}ggq$, $\bar{q}gZq$, $\bar{q}ZZq$, $\bar{q}gggq$, $\bar{q}ggZq$, $\bar{q}gZZq$, and $\bar{q}gggZq$. Here, we use a generic notion of a Z-boson for an external vector particle, but what we really mean are amplitudes with the vector current sandwiched between lepton and antilepton spinors. The relevant tree-level amplitudes can be extracted from different publications; we have mostly benefited from a comprehensive description of helicity amplitudes that involve quarks, gluons, and vector bosons in Ref. [56].

The calculation of the rational part of the $0 \to gggZZ$ amplitude is performed analytically, using techniques suggested in Ref. [50,51]. Similar to the cut-constructable part, the rational amplitude receives contributions from quadruple, triple, and double cuts. However, for the case of $gg \to ZZg$ amplitudes, the double cut contribution vanishes; the rational part, therefore, can be reconstructed from the calculation of boxes and triangles. Unfortunately, even in this case, the analytic results for the rational part are unwieldy, and we choose not to present them here.

For further reference, we give numerical results for the scattering amplitudes below. We consider a kinematic point (momenta are given in GeV),

$$\begin{aligned}
p_1 &= (-238.714576090637, -238.714576090637, 0, 0),\\
p_2 &= (-1021.22119318758, 1021.22119318758, 0, 0),\\
p_3 &= (250.736037681104, -207.896850811885, -124.613643938661, 64.1786550096635),\\
p_4 &= (553.889863453468, -495.644737899924, -245.099246845329, 32.5059044554765),\\
p_5 &= (91.0664644166627, 49.0057636944973, 76.1125676676337, -9.92033815503652),\\
p_6 &= (197.326337775966, -3.11006048502754, 183.877222508616, -71.5344542606618),\\
p_7 &= (166.917065951017, -124.860731594604, 109.723100607740, -15.2297670494417),
\end{aligned} \tag{12}$$

and define a normalized primitive amplitude through the following equation:

$$\mathcal{A}^{LL,RR}_{\mathrm{ijk}}(\lambda_i,\lambda_j,\lambda_k;\lambda_e,\lambda_\mu) = \frac{i}{(4\pi)^2}\times 10^{-9} \times \tilde{\mathcal{A}}^{LL,RR}_{\mathrm{ijk}}(\lambda_i,\lambda_j,\lambda_k;\lambda_e,\lambda_\mu). \tag{13}$$

The results for certain helicity combinations of gluons and leptons are given in Table II. We emphasize that diagrams where one Z-boson is emitted by decay products of another Z-boson, see Fig. 1(b), are *not* included in our calculation. The result for the amplitude squared and summed over colors and helicities of gluons and leptons was checked against the results of the OpenLoops program [38,39] for a large number of kinematic points.[5] Finally, we note that the evaluation of the amplitude squared, summed over color and helicities, takes about 0.1 s per phase-space point, making our implementation adequate for phenomenological needs.

In the context of NLO QCD computations, the process $gg \to ZZ + g$ represents an inelastic contribution. This inelastic contribution should be integrated over all energies and angles of the emitted gluons, including the vanishingly small ones. Calculation of one-loop amplitudes for the $gg \to ZZg$ process becomes unstable if the gluon in the final state becomes soft or collinear to the collision axis. We deal with these instabilities by switching to quadruple

[5]We are indebted to J. Lindert for making this comparison possible.

precision where appropriate. To obtain the $gg \to ZZ$ cross section through NLO QCD, we combine elastic and inelastic contributions using the q_t-subtraction [48] and, as a cross-check, the Frixione-Kunszt-Signer subtraction [57] methods. The results that we present in the next section are obtained by combining computations performed using the two subtraction schemes.

IV. NUMERICAL RESULTS

In this section we present the results of the calculation. We consider the process $gg \to (Z/\gamma)(Z/\gamma) \to e^+e^-\mu^+\mu^-$ at the LHC.[6] We generate invariant masses of Z-bosons around m_Z, using Breit–Wigner distributions. We require the e^+e^- and $\mu^+\mu^-$ pair to have invariant masses $m_{l\bar{l}} \in (60, 120)$ GeV. We use leading- (next-to-leading-) order parton distribution functions and the strong coupling constant for one- and two-loop calculations, respectively. We employ the NNPDF3.0 set of parton distribution functions and obtain the relevant values of the strong coupling constant from NNPDF routines [59].

We begin with presenting the results for the total cross sections at the 8 TeV LHC. We find

$$\sigma_{\rm LO}^{gg\to ZZ} = 0.97^{+0.3}_{-0.2}\ \text{fb}, \qquad \sigma_{\rm NLO}^{gg\to ZZ} = 1.8^{+0.2}_{-0.2}\ \text{fb}, \quad (14)$$

where the central values refer to the renormalization and factorization scales set to $\mu = 2m_Z$ and the upper (lower) values to $\mu = m_Z$ ($\mu = 4m_Z$). It follows from Eq. (14) that QCD corrections to $gg \to ZZ$ are large—the NLO cross section increases the LO cross section by $\mathcal{O}(60\%$–$110\%)$, depending on the renormalization scale. For $\mu = 2m_Z$, the cross section increases by 85%.

A similar situation occurs at the 13 TeV LHC. We find

$$\sigma_{\rm LO}^{gg\to ZZ} = 2.8^{+0.7}_{-0.6}\ \text{fb}, \qquad \sigma_{\rm NLO}^{gg\to ZZ} = 4.7^{+0.4}_{-0.4}\ \text{fb}. \quad (15)$$

The NLO QCD corrections to $gg \to ZZ$ at 13 TeV LHC are again significant but somewhat smaller than corrections at 8 TeV. Indeed, for the central value of the renormalization and factorization scales $\mu = 2m_Z$, the cross section increases by 67%. For other values of the renormalization and factorization scales, the cross section increases by $\mathcal{O}(40\%$–$90\%)$.

The large size of the QCD corrections is reminiscent of the large QCD corrections to Higgs production in gluon fusion $gg \to H$ [60]. In addition, similar to the Higgs production case, the scale variation of the leading-order cross section provides a poor estimate of the magnitude of next-to-leading-order corrections [60]. We note that if we take the proximity of radiative effects in $gg \to ZZ$ and $gg \to H$ seriously we should probably take $\mu = (2m_Z)/2 = m_Z$ as the scale for which higher-order radiative corrections to $gg \to ZZ$ will most likely be small. Thus, our best estimates of $gg \to ZZ$ contributions to the $pp \to ZZ$ production cross section at 8 TeV and 13 TeV LHC are

$$\begin{aligned} \sigma_{pp\to ZZ}^{gg}(8\ \text{TeV}) &= 2.0(2)\ \text{fb}, \\ \sigma_{pp\to ZZ}^{gg}(13\ \text{TeV}) &= 5.1(4)\ \text{fb}. \end{aligned} \quad (16)$$

Our results have important implications for the recently computed NNLO QCD corrections to $pp \to ZZ$ [10,12] at the 8 TeV LHC. In that case, the NNLO QCD corrections computed at the scale $\mu = m_Z$ turned out to be close to 15%. However, a significant fraction—60% of the total NNLO QCD correction—is due to the leading-order contribution $gg \to ZZ$. Our current computation shows that $gg \to ZZ$ receives large radiative corrections, and the natural question is how these findings affect the central value of the $pp \to ZZ$ cross section obtained in Refs. [10,12] and the theory uncertainty assigned to it.

To answer this question, we note that in Refs. [10,12] the central scale was chosen to be $\mu = m_Z$ and that NNLO parton distribution functions were used for the calculation of the $gg \to ZZ$ cross section. Relative to our choices, the lower renormalization and factorization scale increases the cross section, while the choice of NNLO parton distribution functions makes the cross section smaller. We recomputed the LO $gg \to ZZ$ cross section using the setup of Ref. [10] and compared it with our best value given in Eq. (16). We find that, to match our best prediction, the 8 TeV $gg \to ZZ$ cross section of Ref. [10] should be increased by about 80%. In turn, this will lead to an increase in the total NNLO QCD correction to $pp \to ZZ$ at 8 TeV from the current 12%, as calculated in Ref. [10], to 18%. This increase is beyond the $\mathcal{O}(3\%)$ scale variation of the NNLO QCD result for $pp \to ZZ$ used in Ref. [10] to estimate the current uncertainty in the theoretical prediction for the $pp \to ZZ$ cross section. Similar arguments also apply at the 13 TeV LHC. In this case the 16% corrections quoted in Ref. [10] would increase to approximately 23%.

Next, we consider kinematic distributions. We begin with the invariant mass distribution of the four leptons produced in $gg \to ZZ$ shown in Fig. 2. While radiative corrections are significant for all values of m_{4l}, they become smaller at higher values of four-lepton invariant masses. This is clearly seen in Fig. 2 for both differential and cumulative[7] cross sections and for both the 8 TeV and the 13 TeV LHC. This result is important for studies of the Higgs off-shell production where good understanding of the shape of four-lepton invariant mass distribution is an important prerequisite for constraining the Higgs width. Note that for $m_{4l} > 2m_t$ top-quark contributions, neglected in our computation, become relevant.

[6]We remind the reader that we only include double resonant diagrams; see Fig. 1(a). Single resonant diagrams, Fig. 1(b), are only relevant for far off-shell production. They can be obtained by appropriate modifications of the $gg \to Zg$ amplitudes; see e.g. Ref. [58].

[7]For different cuts on m_{4l}.

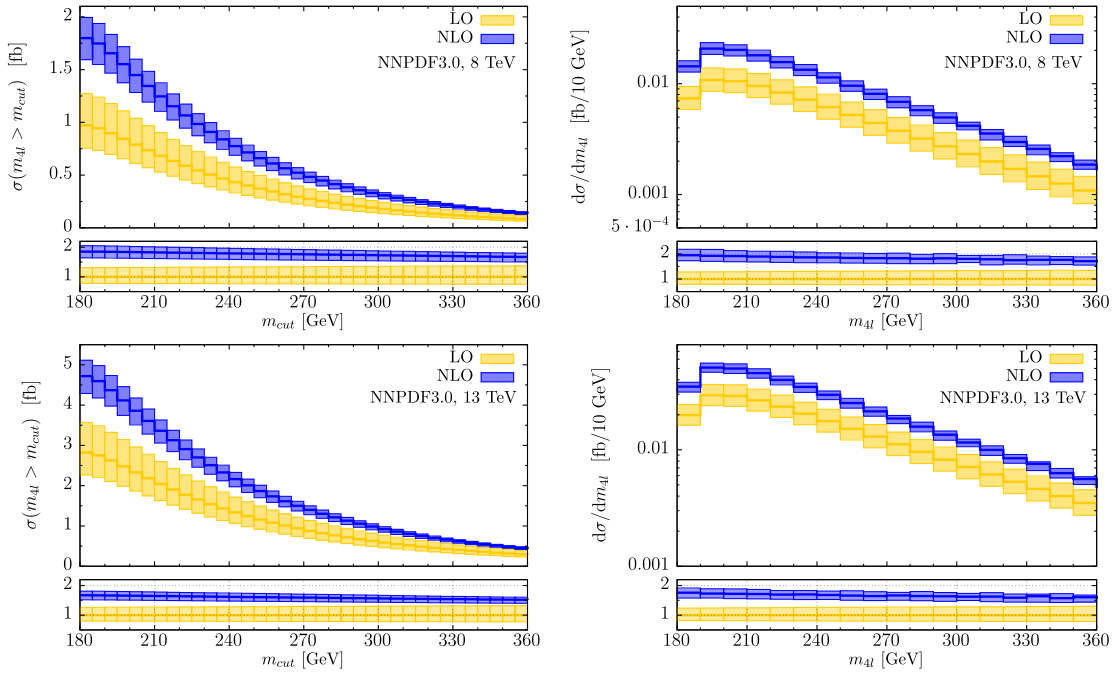

FIG. 2 (color online). Up, left: cumulative cross section for $gg \to (Z/\gamma)(Z/\gamma) \to e^+e^-\mu^+\mu^-$ at the 8 TeV LHC as a function of the lower cut on the four-lepton invariant mass. Up, right: distribution of the invariant mass of the four leptons in the reaction $gg \to (Z/\gamma)(Z/\gamma) \to e^+e^-\mu^+\mu^-$ at the 8 TeV LHC. Lower panes show ratios of the LO (yellow) and NLO (blue) distributions evaluated at three different scales to the LO distribution evaluated at $\mu = 2m_Z$. Low: same as above for the 13 TeV LHC.

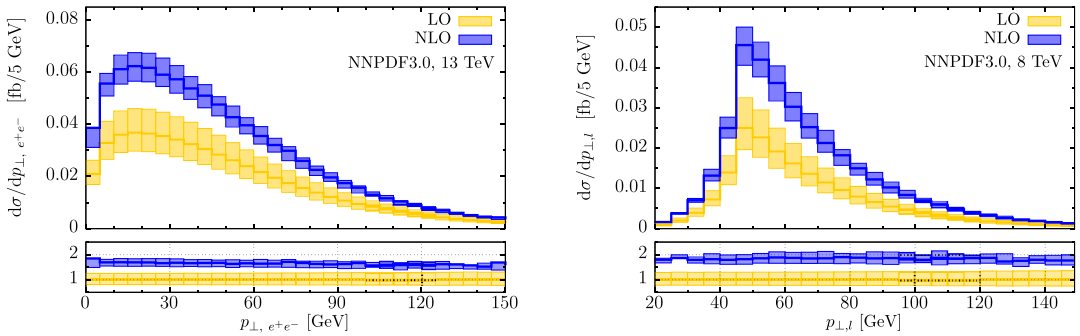

FIG. 3 (color online). Left: transverse momentum distribution of an e^+e^- pair at the 13 TeV LHC. Right: the hardest lepton transverse momentum distribution at the 8 TeV LHC. Lower panes show ratios of the LO (yellow) and NLO (blue) distributions evaluated at three different scales to the LO distribution evaluated at $\mu = 2m_Z$.

In Fig. 3 we show the transverse momentum distributions of the e^+e^- pair and of the hardest lepton in the event. The QCD corrections to the transverse momentum distribution of the e^+e^- pair decrease for large values of $p_{\perp,e^+e^-}$, similar to what is seen in the four-lepton invariant mass distribution. On the other hand, the QCD corrections for the transverse momentum distribution of the hardest lepton are independent of the lepton $p_\perp$.

V. CONCLUSIONS

In this paper we computed QCD corrections to the production of a pair of Z-bosons in gluon fusion through loops of massless quarks. We found that QCD corrections are large; they change the production cross section by almost a factor of 2. These large QCD corrections are in line with expectations that the transition of two gluons to a colorless final state is strongly affected by QCD radiative effects; QCD corrections of similar magnitude were observed earlier in theoretical calculations of $gg \to H$ [60] and $gg \to \gamma\gamma$ [61] cross sections.

Large QCD corrections to $gg \to ZZ$ are important for a number of reasons. First, since the $gg \to ZZ$ process provides a significant fraction of the NNLO QCD contribution to $pp \to ZZ$, our result suggests that existing theoretical predictions for $pp \to ZZ$ should be increased by 6% to 8%, depending on collider energy. Since such an increase in the central value is outside the existing estimates

of the residual theory uncertainty of the $pp \to ZZ$ cross section, it will have important consequences for ongoing comparisons of experimental and theoretical results for $pp \to ZZ$ at the LHC. Second, good understanding of $gg \to ZZ$ at high four-lepton invariant masses is crucial for the so-called off-shell studies of the Higgs boson and, in particular, for the indirect determination of its width. The NLO QCD calculation of the $gg \to ZZ$ process allows us to predict the $gg \to ZZ$ contribution to the $pp \to ZZ$ cross section and kinematic distribution with the precision of about 10%; this implies a residual theoretical uncertainty on the $pp \to ZZ$ cross section of just about 2%. Such a small uncertainty in the four-lepton production cross section is an essential prerequisite for the success of forthcoming off-shell studies of the Higgs boson; see a related discussion in Ref. [7].

As a final comment, we note that our calculation opens up a number of future research directions. Indeed, it is interesting to extend our calculation by combining massless and massive loop contributions to $gg \to ZZ$ and by including single resonant contributions and the interference of prompt $gg \to ZZ$ and $gg \to H^* \to ZZ$ amplitudes. This will allow us to explore the region of four-lepton invariant masses both below the threshold of ZZ production and at very high invariant masses. We plan to do this in the near future.

ACKNOWLEDGMENTS

We are grateful to S. Pozzorini and, especially, to J. Lindert for their help in checking the scattering amplitude for the $gg \to ZZ + g$ process computed in this paper against the implementation in OpenLoops. We would like to thank R. K. Ellis and J. Campbell for useful conversations about the computation of the rational part. F. C. and K. M. thank the Mainz Institute for Theoretical Physics for hospitality and partial support during the program *Higher Orders and Jets for LHC*. This research is partially supported by BMBF Grant No. 05H15VKCCA. Fermilab is operated by Fermi Research Alliance, LLC, under Contract No. De-AC02-07CH11359 with the U.S. Department of Energy.

[1] G. Aad *et al.* (ATLAS Collaboration), Phys. Rev. D **87**, 112001 (2013); **88**, 079906(E) (2013).
[2] S. Chatrchyan *et al.* (CMS Collaboration), Eur. Phys. J. C **73**, 2610 (2013).
[3] CMS Collaboration, Report No. CMS-PAS-SMP-12-013.
[4] V. Khachatryan *et al.* (CMS Collaboration), Eur. Phys. J. C **75**, 212 (2015).
[5] V. Khachatryan *et al.* (CMS Collaboration), Phys. Rev. D **92**, 012004 (2015).
[6] V. Khachatryan *et al.* (CMS Collaboration), Phys. Lett. B **736**, 64 (2014).
[7] G. Aad *et al.* (ATLAS Collaboration), Eur. Phys. J. C **75**, 335 (2015).
[8] S. Catani, L. Cieri, D. de Florian, G. Ferrera, and M. Grazzini, Phys. Rev. Lett. **108**, 072001 (2012).
[9] M. Grazzini, S. Kallweit, D. Rathlev, and A. Torre, Phys. Lett. B **731**, 204 (2014).
[10] F. Cascioli, T. Gehrmann, M. Grazzini, S. Kallweit, P. Maierhöfer, A. von Manteuffel, S. Pozzorini, D. Rathlev, L. Tancredi, and E. Weihs, Phys. Lett. B **735**, 311 (2014).
[11] T. Gehrmann, M. Grazzini, S. Kallweit, P. Maierhoefer, A. von Manteuffel, S. Pozzorini, D. Rathlev, and L. Tancredi, Phys. Rev. Lett. **113**, 212001 (2014).
[12] M. Grazzini, S. Kallweit, and D. Rathlev, J. High Energy Phys. 07 (2015) 085.
[13] M. Grazzini, S. Kallweit, and D. Rathlev, Phys. Lett. B **750**, 407 (2015).
[14] E. W. N. Glover and J. J. van der Bij, Nucl. Phys. **B321**, 561 (1989).
[15] E. W. N. Glover and J. J. van der Bij, Phys. Lett. B **219**, 488 (1989).
[16] D. A. Dicus, C. Kao, and W. W. Repko, Phys. Rev. D **36**, 1570 (1987).
[17] T. Binoth, M. Ciccolini, N. Kauer, and M. Kramer, J. High Energy Phys. 12 (2006) 046.
[18] M. Bonvini, F. Caola, S. Forte, K. Melnikov, and G. Ridolfi, Phys. Rev. D **88**, 034032 (2013).
[19] F. Caola and K. Melnikov, Phys. Rev. D **88**, 054024 (2013).
[20] J. M. Campbell, R. K. Ellis, and C. Williams, J. High Energy Phys. 04 (2014) 060.
[21] N. Kauer and G. Passarino, J. High Energy Phys. 08 (2012) 116.
[22] J. M. Campbell, R. K. Ellis, and C. Williams, J. High Energy Phys. 10 (2011) 005.
[23] A. Azatov, C. Grojean, A. Paul, and E. Salvioni, Zh. Eksp. Teor. Fiz. **147**, 410 (2015); [J. Exp. Theor. Phys. **120**, 354 (2015)].
[24] J. Campbell and R. K. Ellis, http://mcfm.fnal.gov.
[25] N. Kauer, J. High Energy Phys. 12 (2013) 082.
[26] K. Melnikov and M. Dowling, Phys. Lett. B **744**, 43 (2015).
[27] T. Gehrmann, L. Tancredi, and E. Weihs, J. High Energy Phys. 08 (2013) 070.
[28] T. Gehrmann, A. von Manteuffel, L. Tancredi, and E. Weihs, J. High Energy Phys. 06 (2014) 032.
[29] J. M. Henn, K. Melnikov, and V. A. Smirnov, J. High Energy Phys. 05 (2014) 090.
[30] F. Caola, J. M. Henn, K. Melnikov, and V. A. Smirnov, J. High Energy Phys. 09 (2014) 043.
[31] C. G. Papadopoulos, D. Tommasini, and C. Wever, J. High Energy Phys. 01 (2015) 072.
[32] T. Gehrmann, A. von Manteuffel, and L. Tancredi, J. High Energy Phys. 09 (2015) 128.

[33] F. Caola, J. M. Henn, K. Melnikov, A. V. Smirnov, and V. A. Smirnov, J. High Energy Phys. 11 (2014) 041.
[34] F. Caola, J. M. Henn, K. Melnikov, A. V. Smirnov, and V. A. Smirnov, J. High Energy Phys. 06 (2015) 129.
[35] A. von Manteuffel and L. Tancredi, J. High Energy Phys. 06 (2015) 197.
[36] P. Agrawal and A. Shivaji, Phys. Rev. D **86**, 073013 (2012).
[37] F. Campanario, Q. Li, M. Rauch, and M. Spira, J. High Energy Phys. 06 (2013) 069.
[38] F. Cascioli, P. Maierhofer, and S. Pozzorini, Phys. Rev. Lett. **108**, 111601 (2012).
[39] OpenLoops is a one-loop generator by F. Cascioli, J. Lindert, P. Maierhöfer, and S. Pozzorini, http://openloops.hepforge.org.
[40] V. Hirschi and O. Mattelaer, J. High Energy Phys. 10 (2015) 146.
[41] Z. Bern, L. J. Dixon, and D. A. Kosower, Nucl. Phys. **B513**, 3 (1998).
[42] R. Britto, F. Cachazo, and B. Feng, Nucl. Phys. **B725**, 275 (2005).
[43] G. Ossola, G. G. Papadopoulos, and R. Pittau, Nucl. Phys. **B763**, 147 (2007).
[44] R. K. Ellis, W. T. Giele, and Z. Kunszt, J. High Energy Phys. 03 (2008) 003.
[45] W. T. Giele, Z. Kunszt, and K. Melnikov, J. High Energy Phys. 04 (2008) 049.
[46] R. K. Ellis, Z. Kunszt, K. Melnikov, and G. Zanderighi, Phys. Rep. **518**, 141 (2012).
[47] J. M. Henn and J. C. Plefka, Lect. Notes Phys. **883**, 1 (2014).
[48] S. Catani and M. Grazzini, Phys. Rev. Lett. **98**, 222002 (2007).
[49] S. Catani, L. Cieri, D. de Florian, G. Ferrera, and M. Grazzini, Nucl. Phys. **B881**, 414 (2014).
[50] S. Badger, J. High Energy Phys. 01 (2009) 049.
[51] J. M. Campbell, R. K. Ellis, E. Furlan, and R. Rontsch, Phys. Rev. D **90**, 093008 (2014).
[52] R. K. Ellis, W. T. Giele, Z. Kunszt, K. Melnikov, and G. Zanderighi, J. High Energy Phys. 01 (2009) 012.
[53] T. Melia, K. Melnikov, R. Rontsch, and G. Zanderighi, J. High Energy Phys. 12 (2010) 053.
[54] T. Melia, K. Melnikov, R. Rontsch, and G. Zanderighi, Phys. Rev. D **83**, 114043 (2011).
[55] T. Melia, K. Melnikov, R. Rontsch, M. Schulze, and G. Zanderighi, J. High Energy Phys. 08 (2012) 115.
[56] S. D. Badger, E. W. N. Glover, and V. Khoze, J. High Energy Phys. 01 (2006) 066.
[57] S. Frixione, Z. Kunszt, and A. Signer, Nucl. Phys. **B467**, 399 (1996).
[58] T. Gehrmann, L. Tancredi, and E. Weihs, J. High Energy Phys. 04 (2013) 101.
[59] R. D. Ball *et al.* (NNPDF Collaboration), J. High Energy Phys. 04 (2015) 040.
[60] Graudenz, M. Spira, and P. M. Zerwas, Phys. Rev. Lett. **70**, 1372 (1993); S. Dawson, Nucl. Phys. **B359**, 283 (1991); A. Djouadi, M. Spira, and P. M. Zerwas, Phys. Lett. B **264**, 440 (1991); M. Spira, A. Djouadi, D. Graudenz, and P. M. Zerwas, Nucl. Phys. **B453**, 17 (1995); R. V. Harlander and W. B. Kilgore, Phys. Rev. Lett. **88**, 201801 (2002); C. Anastasiou and K. Melnikov, Nucl. Phys. **B646**, 220 (2002); V. Ravindran, J. Smith, and W. L. van Neerven, Nucl. Phys. **B665**, 325 (2003); C. Anastasiou, C. Duhr, F. Dulat, F. Herzog, and B. Mistlberger, Phys. Rev. Lett. **114**, 212001 (2015).
[61] Z. Bern, L. J. Dixon, and C. Schmidt, Phys. Rev. D **66**, 074018 (2002).